

Soft x-ray pumping of metastable levels of Li^+

R. G. Caro, J. C. Wang, R. W. Falcone, J. F. Young, and S. E. Harris
Edward L. Ginzton Laboratory, Stanford University, Stanford, California 94305

(Received 9 July 1982; accepted for publication 5 October 1982)

Soft x rays from a plasma generated by a neodymium: yttrium aluminum garnet laser beam ($1.06 \mu\text{m}$) are used to photoionize neutral Li vapor to produce Li^+ metastables. Maximum metastable densities of $\text{Li}^+ (1s2s) ^1S = 6 \times 10^{14}$ ions/ cm^3 and $\text{Li}^+ (1s2s) ^3S = 3 \times 10^{15}$ ions/ cm^3 are obtained. The effective lifetimes of these levels are measured to be approximately 5 ns. At 50 mJ of incident laser energy the inferred conversion efficiency from $1.06\text{-}\mu\text{m}$ radiation to soft x rays is $\sim 14\%$.

PACS numbers: 42.60.Kg, 52.50.Jm, 32.30.Rj, 32.80.Fb

Recent proposals for the construction of soft x-ray lasers^{1,2} and tunable XUV radiation sources³ are based on obtaining high densities of metastable $(1s2s) ^1S$ lithium ions (66 eV). Using pulsed high power microwave discharges⁴ and hollow cathode discharges,⁵ metastable singlet densities of about 10^{11} ions/ cm^3 and 2×10^{12} ions/ cm^3 , respectively, have been created. In this letter we describe the production of Li^+ metastables by inner-shell photoionization^{6,2} of neutral Li by means of soft x rays which are emitted from a plasma⁷⁻⁹ produced by the focused beam from a neodymium: yttrium aluminum garnet (Nd:YAG) laser ($1.06 \mu\text{m}$). Over a length of a few millimeters, metastable $(1s2s) ^1S$ densities as high as 6×10^{14} ions/ cm^3 have been obtained.

The configuration of the experiment described here is shown in Fig. 1. A massive plane target was placed inside a heat pipe containing lithium vapor at a density which could vary from 10^{16} to 10^{17} atoms/ cm^3 . The $1.06\text{-}\mu\text{m}$ laser beam was focused onto the tantalum target by a lens of 12-cm focal length with an effective f number of $f/8$. For an intensity of 1×10^{13} W/ cm^2 of $1.06\text{-}\mu\text{m}$ radiation on the target, the conversion efficiency from incident laser energy to energy of soft x rays emitted from the laser-produced plasma was estimated to be $\sim 14\%$. The emitted soft x-ray radiation propagated into the surrounding Li vapor causing inner-shell photoionization and therefore production of metastable $(1s2s) ^1S$ and $(1s2s) ^3S$ Li^+ ions. For 70-eV radiation the cross section for photoionization¹⁰ of Li atoms is 3×10^{-18} cm^2 . Therefore, at a vapor density of 10^{17} atoms/ cm^3 , the stopping distance for soft x rays is about 3 cm.

The metastable $\text{Li}^+ (1s2s) ^1S$ and $\text{Li}^+ (1s2s) ^3S$ population densities were determined by measuring the absorption of laser probe beams as a function of wavelength at the $\text{Li}^+ [(1s2s) ^1S - (1s2p) ^1P]$ and $\text{Li}^+ [(1s2s) ^3S - (1s2p) ^3P]$ transitions at 958.1 and 548.5 nm (Fig. 2). The absorption traces were fitted to numerically generated Voigt profiles using the oscillator strengths and Doppler and Lorentzian linewidths shown in the insert in Fig. 2. The integral of metastable population over length along the probe beam, which in the following is defined as $N * L$, was measured as a function of laser energy, time delay between the $1.06\text{-}\mu\text{m}$ pulse and the probe pulse, and as a function of the distance of the probe from the target surface.

The $1.06\text{-}\mu\text{m}$ laser consisted of an actively mode-locked Nd:YAG oscillator,¹¹ a Pockels cell pulse selector, and three Nd:YAG rod amplifiers with a final aperture of 6-mm diameter. The output beam had a maximum energy of 100 mJ of

which 70% was contained in a main pulse with a measured duration of 600 ps. Leakage through the Pockels cell resulted in a prepulse and two post pulses, each separated by 4 ns, 600 ps long, and containing $\sim 10\%$ of the total pulse energy. The laser operated at a repetition rate of two pulses per second.

Using a scanning knife edge, the beam radius in the focal plane and the effective confocal parameter were measured. At a total laser energy of 50 mJ these were $w_0 \cong 20 \mu\text{m}$ and $b \cong 900 \mu\text{m}$. An approximate calculation suggests that passage through the Li vapor should not result in significant distortion of the laser beam. In this case the measured beam parameters imply a peak on-target intensity in the main pulse of approximately 10^{13} W/ cm^2 . It should be noted that the measured values of $N * L$ changed by little more than a factor of 2 when the focusing lens was translated by ± 3 mm, even though the estimated intensity at the target changed by a factor of about 40.

Since the tantalum target was located inside a lithium heat pipe ($\sim 900^\circ\text{C}$), it was initially uncertain whether the target was Ta or liquid Li condensed onto the tantalum. The emission spectrum from a laser-generated plasma produced on a cold clean tantalum target was examined with a McPherson grazing incidence spectrometer over the region from 15 to 65 nm. At a spectrometer resolution of 0.2 nm the emission appeared to be a continuum. As the cell temperature was raised the spectrum was re-examined and no change in the plasma emission was observed. However, several absorption lines were observed which could be assigned to autoionizing transitions in the neutral lithium atoms which

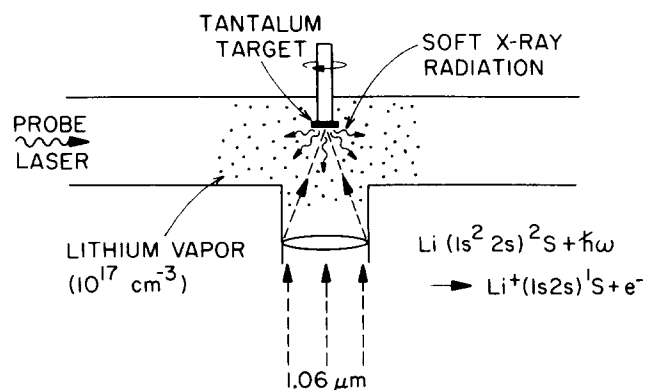


FIG. 1. Schematic of experimental configuration.

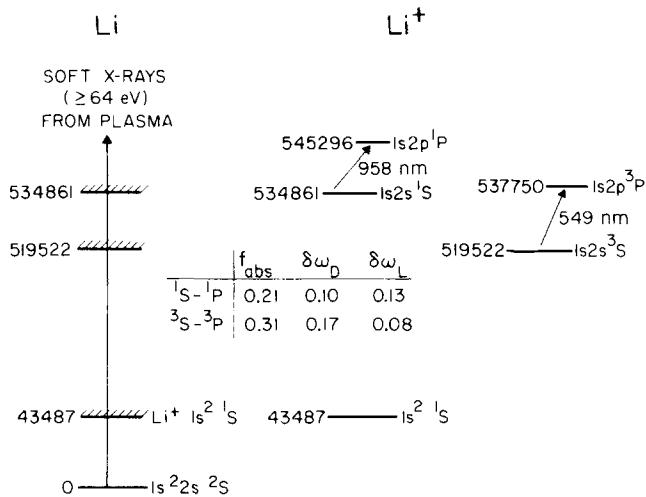


FIG. 2. Energy-level diagram for inner-shell photoionization and laser absorption probes. The inset table shows oscillator strengths and Doppler and Lorentzian linewidths ($\delta\omega_D$, $\delta\omega_L$) of the $1S-1P$ and $3S-3P$ transitions in Li^+ . The units of linewidth are cm^{-1} . The energy levels are expressed in cm^{-1} .

were contained in the cell between the laser-produced plasma and the spectrometer. The cell was then cooled down and the tantalum target replaced by solid Li. In this case the plasma emission spectrum contained predominantly line radiation and was two orders of magnitude less intense than for the Ta target. These observations lead us to believe that the participating target was tantalum and not liquid Li.

To prevent excessive target destruction, the target was rotated between laser shots. However, after one revolution of the target ($\sim 70^\circ$ laser shots) a circular groove corresponding to regions of plasma ablation was formed on the target and, for subsequent shots, the laser was focused into this groove. It seems likely that the formation of the plasma in a depression on the target resulted in a nonisotropic distribution of x-ray emission. In the remainder of this work it will be assumed that the x rays emitted from the plasma had the radiation pattern of a cone with half-angle 45° and an axis normal to the target.

Figure 3 shows the measured value of integrated Li^+ ($1s2s$) $1S$ metastable population, N^*L , as a function of the total laser energy incident on the target. The laser probe beam at 958.1 nm [$(1s2s) 1S-(1s2p) 1P$] was obtained by Raman downshifting the pulsed 685.2-nm output of a Quanta-Ray dye laser. The Li vapor density for this experiment was $\sim 10^{17}$ atoms/ cm^3 . The laser probe beam had a diameter of 2 mm and was centered about 1 mm from the Ta target (Fig. 1). Assuming a 45° conical soft x-ray radiation pattern, the maximum measured value of N^*L from Fig. 3 implies a singlet metastable population of 3×10^{14} ions/ cm^3 . If an isotropic radiator is assumed this value is reduced by a factor of 2. It can be seen from Fig. 3 that the conversion efficiency from incident 1.06- μm laser energy to soft x-ray energy in the 66–150-eV photoabsorption band continues to increase as the laser energy is increased.

The dependence of N^*L on the Li vapor density was studied and N^*L was found to increase monotonically up to the maximum obtainable density of 10^{17} Li atoms/ cm^3 . As

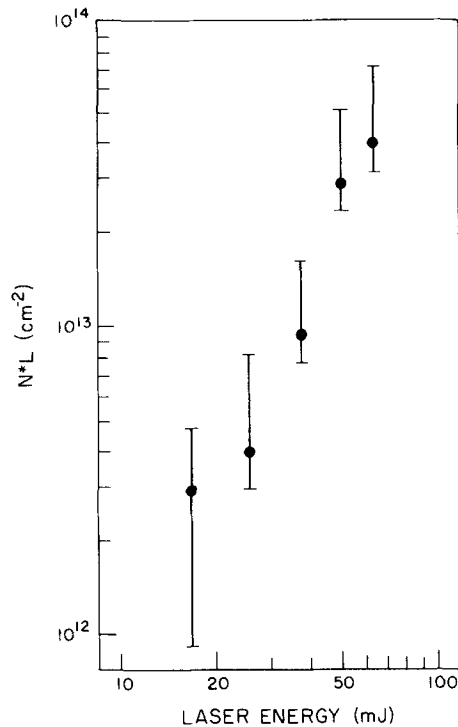


FIG. 3. Integrated metastable density N^*L , for Li^+ ($1s2s$) $1S$ vs total laser energy incident on the target. Li vapor density = $10^{17}/\text{cm}^3$. The perpendicular probe-target distance is $R = 1$ mm. The time delay between the peaks of the probe and 1.06- μm lasers is ~ 4 ns.

expected from geometrical considerations, the dependence of N^*L on the perpendicular distance, R , of the 2-mm-diam probe beam from the target varied approximately as $1/R$ for $R \geq 1$ mm.

Figure 4 shows the results of a measurement of N^*L for metastable Li^+ singlets as a function of the time delay, t , between the peaks of the 958.1-nm probe pulse and the 1.06- μm laser pulse incident on the Ta target. The time origin in Fig. 4 has an experimental uncertainty of ± 2 ns. The slope of the graph of Fig. 4 corresponds to a singlet metastable ($1/$

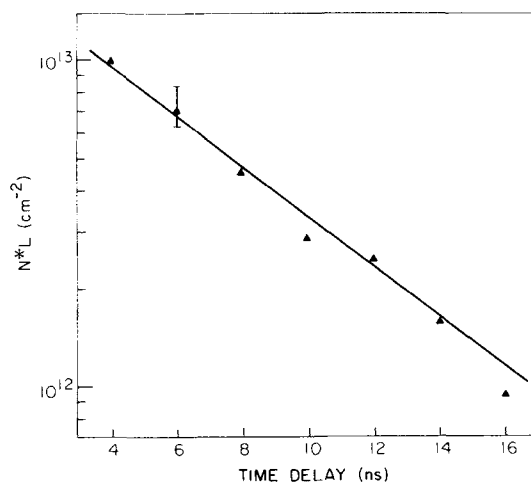


FIG. 4. N^*L for Li^+ ($1s2s$) $1S$ vs the time delay between the peaks of the probe laser and the 1.06 μm laser. Li vapor density = $10^{17}/\text{cm}^3$; total incident laser energy = 50 mJ; $R = 4.5$ mm.

e) decay time of 5.3 ns. Such a decay time is consistent with calculated rates¹ for destruction of Li⁺ metastable ions due to collisions with electrons. At a probe-target distance of $R = 1$ mm the $(1s2s) {}^1S$ decay time was measured to be 3.6 ns. This change in decay time is to be expected in view of the higher electron density at $R = 1$ mm than at $R = 4.5$ mm where the results of Fig. 4 were obtained. It should be noted that for the values of R and t investigated here ($R \geq 1$ mm; $4 \leq t \leq 16$ ns) there was no evidence from our experiments that suggested any effects due to interaction of the metastable Li⁺ ions with either the plasma expanding from the target or a precursor ionization front.¹²

The above results may be summarized by the expressions

$$N^*L = [A/R] \exp(-t/\tau), \quad (1a)$$

$$N^* = [B/R^2] \exp(-t/\tau), \quad (1b)$$

with N^* , L , and R having units of cm^{-3} , cm, and cm respectively. For metastable Li⁺ $(1s2s) {}^1S$ ions, $A = 10^{13}$ ions/cm, $B = 6 \times 10^{12}$ ions/cm, and τ varies from 4–5 ns as R increases from 1 to 5 mm. The uncertainties in A and B are $\pm 50\%$. While Eq. (1a) can be deduced directly from the measured values of N^*L , the value of B in Eq. (1b) is dependent on the assumption of a particular radiation pattern for the soft x-ray emission. We have assumed conical emission with a half-angle of 45° . Similar measurements were made on metastable Li⁺ $(1s2s) {}^3S$ ions. Here it was found, with a comparable error, that $A = 4 \times 10^{13}$ ions/cm, $B = 3 \times 10^{13}$ ions/cm, and $\tau = 6$ ns at $R = 2$ mm. Although measurements were taken only for $t \geq 4$ ns, it seems reasonable to extrapolate Eqs. (1a) and (1b) to $t = 0$.

One may use the value of N^* at a given R to estimate the conversion efficiency from incident $1.06\text{-}\mu\text{m}$ energy to soft x-ray energy. To obtain a lower limit for this conversion efficiency a soft x-ray spectral distribution well matched to the Li photoabsorption spectral profile should be postulated. For this reason a spectral distribution characteristic of a 30-eV blackbody was assumed here. We take the peak cross section for photoionization of Li atoms to produce Li⁺ singlet metastables¹⁰ to be $7 \times 10^{-19} \text{ cm}^2$ and the spectrally averaged cross section to be $2 \times 10^{-19} \text{ cm}^2$. Based on extrapolation of the measured singlet population to $t = 0$, we estimate the conversion efficiency to be $(14 \pm 7)\%$. This estimate must be increased if a less optimum spectral distribution, or a more isotropic spatial distribution, is assumed. The high conversion efficiencies observed in this work are comparable to those reported elsewhere⁸ and are believed to result from a combination of the large atomic weight of the target material and the relatively low input laser intensities and long pulse durations used.

By comparison with results obtained elsewhere⁸ the as-

sumed plasma radiation temperature of 30 eV would be expected to prevail at incident laser intensities of less than 10^{12} W/cm^2 . At the plasma blow off velocities typical of laser-produced plasmas ($10^4\text{--}10^5 \text{ m/s}$)^{9,12} it would be expected that heated plasma would move out of the $20\text{-}\mu\text{m}$ laser focal spot in a time shorter than the duration of the laser pulse. It thus seems likely that for the small laser focal spot size used in this work higher incident intensities ($\sim 10^{13} \text{ W/cm}^2$) were required than would have been predicted by comparison with experiments⁸ in which larger focal spot sizes were involved. This effect would also explain the relative insensitivity, mentioned above, of the measured value of N^*L of Li⁺ $(1s2s) {}^1S$ to translation of the focusing lens normal to the target.

The relatively modest size (50 mJ) of the laser used in this work suggests that the technique used here should be widely applicable to the production of a variety of excited ionic species. This should allow the convenient study of a number of soft x-ray laser proposals as well as the development of new spectroscopic techniques.

The authors take pleasure in acknowledging helpful discussions with R. L. Byer, K. R. Manes, G. H. McCall, D. J. Nagel, and D. W. Phillion, and the technical assistance of Ben Yoshizumi. The work described here was supported by the Office of Naval Research. R. G. Caro and R. W. Falcone wish to gratefully acknowledge the support of an IBM Postdoctoral Fellowship and the Marvin Chodorow Fellowship, respectively.

¹S. A. Mani, H. A. Hyman, and J. D. Daugherty, *J. Appl. Phys.* **47**, 3099 (1976); H. A. Hyman and S. A. Mani, *Opt. Commun.* **20**, 209 (1977).

²S. E. Harris, J. F. Young, R. W. Falcone, Joshua E. Rothenberg, J. R. Willison, and J. C. Wang, in *Laser Techniques for Extreme Ultraviolet Spectroscopy*, edited by R. R. Freeman and T. J. McIlrath (AIP, New York, 1982) (to be published); J. R. Willison, R. W. Falcone, J. C. Wang, J. F. Young, and S. E. Harris, *Phys. Rev. Lett.* **44**, 1125 (1980).

³Joshua E. Rothenberg, J. F. Young, and S. E. Harris, *Opt. Lett.* **6**, 363 (1981).

⁴J. R. Willison, R. W. Falcone, J. F. Young, and S. E. Harris, *Phys. Rev. Lett.* **47**, 1827 (1981).

⁵R. W. Falcone and K. D. Pedrotti, *Opt. Lett.* **7**, 74 (1982).

⁶M. A. Duguay and P. M. Rentzepis, *Appl. Phys. Lett.* **10**, 350 (1967).

⁷M. D. Rosen, D. W. Phillion, V. C. Rupert, W. C. Mead, W. L. Kruer, J. J. Thomson, H. N. Kornblum, V. W. Slivinsky, G. J. Caporaso, M. J. Boyle, and K. G. Tirsell, *Phys. Fluids* **22**, 2020 (1979).

⁸H. Nishimura, F. Matsuoka, M. Yagi, K. Yamada, H. Niki, T. Yamanaka, C. Yamanaka, and G. H. McCall, in *Low Energy X-Ray Diagnostics—1981*, edited by D. T. Attwood and B. L. Henke (AIP, New York, 1981), p. 261.

⁹P. K. Carroll and E. T. Kennedy, *Contemp. Phys.* **22**, 61 (1981).

¹⁰G. Mehlman, J. W. Cooper, and E. B. Saloman, *Phys. Rev. A* **25**, 2113 (1982).

¹¹D. J. Kuizenga, *IEEE J. Quantum Electron* **QE-17**, 1694 (1981).

¹²D. W. Koopman, *Phys. Fluids* **15**, 1959 (1972).